Fracture analysis of NiTi Alloys by Finite Element Method

A. Falvo[1,a], F. Furgiuele[1,b], A. Leonardi[1,c] and C. Maletta[1,d]

[1]Mechanical Engineering Department, University of Calabria, 87036 Arcavacata di Rende, Italy

[a]andrea.falvo@unical.it, [b]furgiuele@unical.it, [c]leonardi@unical.it, [d]carmine.maletta@unical.it

Keywords: Shape Memory Alloys (SMAs), NiTi alloys, stress-induced martensitic transformation (SIM), fracture, cracks, finite element analyses.

Abstract. The evolution of stress induced martensitic transformation in front of the crack tip in a Nickel Titanium based shape memory alloy is numerically analyzed in this investigation. To this purpose, 2-D finite element simulations of single edge-crack specimens were carried out, and the effects of the temperature on the martensitic transformation zone as well as on the stress-strain distributions in the crack tip region were analyzed. In particular, the transformation start and finish contours, *i.e.* the boundaries of the transformation zone, were obtained by using plasticity concepts, and the effects of the temperature were taken into account by using the Clausius-Clapeyron relation. The results show that both the extents of the transformation start and finish contours decrease with increasing the temperature; however, the former decreases more rapidly than the latter, resulting in an overall reduction of the transformation zone with increasing the temperature. Finally, comparisons between numerical and analytical results, obtained by modified linear elastic fracture mechanics relations, were carried out. These comparisons show that the analytical approach is able to describe the stress field in the crack tip region outside the phase transformation zone, *i.e.* in the austenitic region.

Introduction

In recent years, shape memory alloys (SMAs), and in particular the Nickel Titanium based ones (NiTi), have received much attention from scientific and engineering communities, owing to their unique characteristics, namely shape memory effect (SME) and superelastic effect (SE) [1]. In particular, these properties allow large recoverable strains or large induced internal forces due to a reversible solid state phase transformation between austenite and martensite; this transformation can be activated by a temperature change (TIM, Thermally Induced Martensite) or by the application of external forces (SIM, Stress Induced Martensite). Due to these interesting features, as well as to their good mechanical performances and biocompatibility, NiTi alloys have seen growing use in the last years in many braches of engineering and medicine. As a direct consequence of this interest many researchers have studied the thermo-mechanical behavior of SMAs, in terms of both SME and SE [1], and various numerical models have been developed in order to describe their mechanical and functional behavior [2]. Unfortunately, a limited number of works have been devoted to the study of the fatigue [3-6] and, above all, fracture behavior [7-11] of NiTi alloys. From materials science point of view an accurate knowledge of these topics is essential in order to predict the failure modes of damaged structures as well as their functional and structural life, with the aim to improve the overall performances of NiTi based components or structures. The fracture behavior of austenitic NiTi alloys strongly depends on the stress induced martensitic transformation (SIM) which occurs in the crack tip region as a consequence of the high values of local stresses.
In an experimental investigation of fracture mechanics in NiTi alloys [11], it has been shown that the crack is stress control propagated in line with the direction of the maximum normal stress. In addition, it was observed that the notch geometries and the martensitic transformation play significant roles on the fracture process of SMAs. In the last years, some finite element analyses concerning the martensitic transformation in front of notches or cracks have been conducted [12,13]; in particular, it has been found that the shape of the martensitic transformation zone at the

crack tip is similar to the characteristic shape of plastic zone for metals. This means that modified plasticity concepts can be used to control the transformation zone in SMAs.
In the present work, two-dimensional (2-D) numerical simulations were carried out in order to investigate the effects of the temperature on the stress-strain distributions and on the martensitic transformation zone in front of the crack tip in a single edge-crack (SEC) specimen. Furthermore, the numerically obtained stress field in the crack tip region was compared with the predictions of modified linear elastic fracture mechanics relations. These comparisons show that the analytical approach is able to describe the stress field outside the phase transformation zone, *i.e.* in the austenitic region.

Constitutive model

The solid piecewise line in Fig. 1 shows a simplified isothermal stress-strain curve for austenitic NiTi based shape memory alloys. It's worth noting that this curve is relative to a monotonically increasing loading path, while if the load is decreased before failure the material exhibits the typical stress-strain hysteretic behavior, as the unloading path is represented by the dashed line in Fig. 1. For the sake of simplicity, in the figure the stress-strain relation is approximated with a piecewise linear curve. The figure clearly shows that, when the applied load is increased, the stress induced martensite transformation (A→M) starts as σ reaches a critical value σ_s^{AM}, and the transformation is completed when σ is equal to σ_f^{AM}, *i.e.* the martensite fraction ξ_M increases from 0 to 1. When unloading, the reverse transformation (M→A) occurs in the stress range σ_s^{MA}-σ_f^{MA}, resulting in a stress-strain hysteretic behavior. However, unloading and the corresponding reverse transformation (martensite to austenite) are not taken into account in this investigation since, for fracture purposes, the specimens for toughness measurements are generally loaded to fracture without unloading.

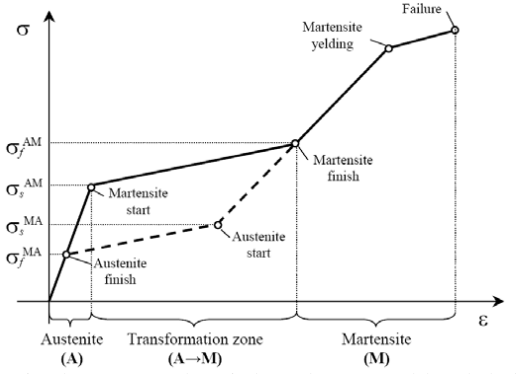

Fig. 1 Classic stress-strain relation of an austenitic NiTi alloy.

The constitutive relation of a Ni-49 at.% Ti alloy were experimentally obtained in a previous work of the authors [14] by isothermal uniaxial tensile tests carried out at several values of the temperature, ranging from 303 K to 328 K. As well known, the stress-strain curves are strongly dependent on the test temperature T, *i.e.* the critical stresses for stress induced transformation change significantly, according to the Clausius-Clapeyron relation:

$$\frac{d\sigma}{dT} = \text{cost.} \tag{1}$$

Let C^{AM} be the constant governing the austenite-to-martensite transformation, then the critical stress values can be obtained as follows:

$$\begin{cases}\sigma_s^{AM} = \sigma_{s0}^{AM} + C^{AM}(T - T_0) \\ \sigma_f^{AM} = \sigma_{f0}^{AM} + C^{AM}(T - T_0)\end{cases}, \tag{2}$$

in which the subscript 0 is referred to the quantities measured at the reference temperature (T_0=303K). The values of C^{AM}, σ_{s0}^{AM} and σ_{f0}^{AM} for the investigated NiTi alloy, together with the Young's moduli and the Poisson's ratios, are reported in Table 1.

Table 1. Thermo-mechanical parameters of a Ni-49 at.% Ti alloy.

E_A [MPa]	ν_A	E_M [MPa]	ν_M	σ_{s0}^{AM} [MPa]	σ_{f0}^{AM} [MPa]	C^{AM} [MPa K^{-1}]
39000	0.3	20000	0.3	260	618,4	10,3

From data in Table 1, and applying Eqs. 2, it is possible to obtain the isothermal stress-strain curves of the NiTi alloy at any temperature, as shown in Fig. 2, in which ε_L, namely the strain increment due to the martensitic phase transformation, was fixed to 7%.

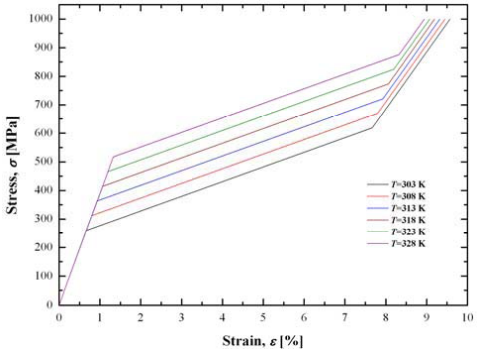

Fig. 2 The piecewise linear stress-strain relation of the NiTi alloy at several temperatures.

As the size of the transformation zone in the crack tip region is expected to be much greater than the plastic zone of the martensitic structure, the curves in Fig. 2 were truncated at a maximum stress equal to 1000 MPa, *i.e.* the yielding of martensite was not modeled.

The martensite volume fraction, ξ_M, during the SIM, can be described by the equivalent plastic strain $\varepsilon_{eq}{}^p$ [13]. Indeed, the yielding condition for a conventional material is:

$$\sigma_{eq} = Y_p(\varepsilon_{eq}{}^p), \tag{3}$$

while the condition for phase transformation in a SMA is:

$$\sigma_{eq} = Y_M(\xi_M), \tag{4}$$

in which σ_{eq} is the von-Mises equivalent stress, while Y_p and Y_M are the plastic and transformation hardening function, respectively. Comparing Eqs. 3 and 4, it can be found that the transformation condition in SMAs is the same as the plastic yield condition in common metals; thus, a simple linear relation between ξ_M and $\varepsilon_{eq}{}^p$ can be assumed [15], that is:

$$\xi_M = C\varepsilon_{eq}{}^p, \tag{5}$$

where C is a constant, which can be easily obtained from the uniaxial stress-strain relation of the SMA. In fact, at the beginning of phase transformation, the martensitic fraction and the equivalent

plastic strain are zero, while at the end of the transformation the martensitic fraction is 1 and the equivalent plastic strain is given by:

$$\varepsilon_{eq}{}^{p} = \varepsilon_{eq} - \varepsilon_{eq}{}^{el} = \varepsilon_{eq} - \frac{\sigma_{eq}}{E_A}, \tag{6}$$

in which ε_{eq} and $\varepsilon_{eq}{}^{el}$ are the total and elastic equivalent strain, respectively. For the piecewise linear stress-strain relations used herein, ε_L and C^{AM} are constant, thus the equivalent plastic strain value at the end of the transformation is also constant and equals to 6,08 10^{-2}. Substituting these values into Eq. (5):

$$C = \frac{\xi_M}{\varepsilon_{eq}{}^{p}} = \frac{1}{6{,}08\,10^{-2}} \approx 16{,}44\,. \tag{7}$$

Therefore, the distributions of martensite volume fraction ξ_M in front of the crack tip can be obtained by the distributions of the equivalent plastic strain $\varepsilon_e{}^{p}$ through the following equation:

$$\xi_M = 16{,}44\,\varepsilon_{eq}{}^{p}\,. \tag{8}$$

Numerical model

A single edge-crack specimen was analyzed by two-dimensional plane stress FE analyses carried out with the commercial finite element code MSC Marc®. The geometry and the dimensions of the SEC specimen are illustrated in Fig. 3, while Fig. 4 shows the corresponding FE model.

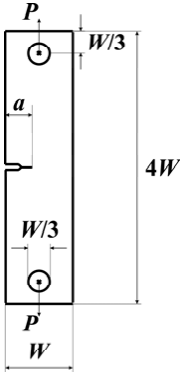

Dimensions [mm]	
Width, W	17,60
Crack length, a	6,80
Thickness, t	1,00

Fig. 3 SEC specimen geometry and dimensions (in millimeters).

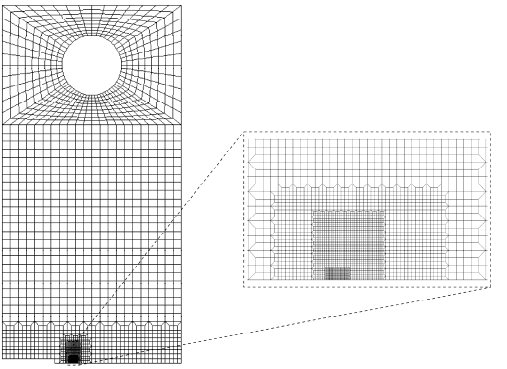

Fig. 4 FE model of the SEC specimen.

Due to the symmetry of the SEC specimen, only one half of the whole specimen was modeled. The model consists of 5629 eight-nodes bi-quadratic plane stress quadrilateral elements. A non-uniform mesh was introduced by employing a relatively fine mesh in the crack tip region, and a coarse mesh away from these critical zones, as clearly shown in Fig. 4.
The tensile load is applied on the upper half of the hole. As previously explained, unloading and the corresponding reverse transformation processes, from martensite to austenite, are not taken into account. The effects of the temperature on the stress-strain distributions and on the evolution of martensitic transformation zone in front of the crack tip in a SEC specimen were investigated.

Results and discussions

The FE model was initially validated by comparing the piecewise linear constitutive model with the numerically obtained equivalent stress-strain, σ_{eq}-ε_{eq}, curve for an applied nominal stress $\sigma^{\infty} = P/(tW) = 20$ MPa. In fact, like plasticity in common metals, the A→M phase transformation is assumed to start when the von-Mises equivalent stress, σ_{eq}, reaches the σ_s^{AM} critical value and is completed when $\sigma_{eq} = \sigma_f^{AM}$. Figure 5 shows excellent agreement between the piecewise linear constitutive relation and numerical results for the temperature T=303 K.

In Fig. 6 the outer and the middle contours represent martensite start, r_A, and finish, r_M, respectively, while the inner one, occurring at 1000 MPa, represents the fixed maximum allowable stress contour. As expected, the figure clearly shows that the size of the transformation zone is much greater than the zone limited by the condition σ_{eq}=1000 MPa.

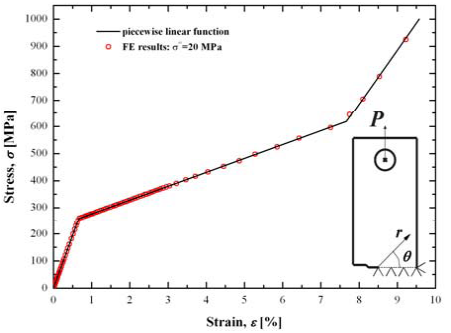

Fig. 5 The piecewise linear constitutive relation and the FEM results (T=303 K).

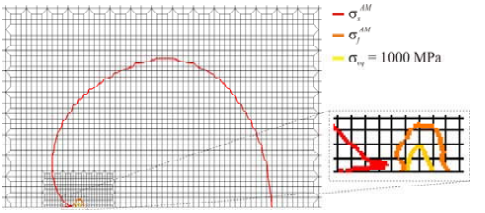

Fig. 6 Martensite start (red), finish (orange) and σ_{eq}=1000 MPa (yellow) contours (T=303 K).

Using Eq. 8, the martensite volume fraction ξ_M in the crack tip region was computed and the results at T=303 K are shown in Fig. 7. The results are presented by the contour lines with constant ξ_M values. The martensite volume fraction ξ_M in the partial martensite zone decreases with increasing the distance from the crack tip. Similar results have been obtained for all the investigated temperatures. In Fig. 8, the trends of r_A and r_M, on the symmetry plane, *i.e.* for $\theta = 0$, *versus* temperature are shown. Both the sizes of the transformation start and finish regions decrease with increasing the temperature; however, the size of the transformation start contour decreases more rapidly with respect to the finish one, resulting in an overall reduction of the transformation zone, which is represented by the gapping area between the curves in Fig. 8.

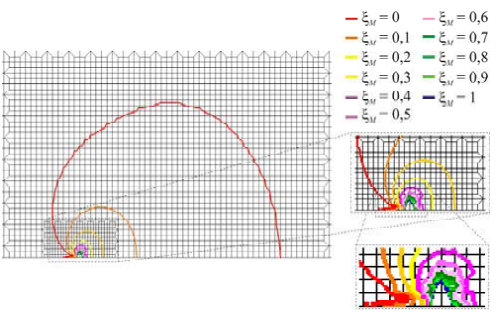

Fig. 7 Contour lines of constant martensite volume fraction ξ_M (T=303 K).

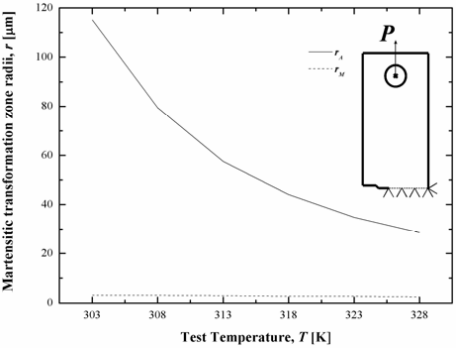

Fig. 8 Martensitic transformation zone *vs*. test temperature, T.

As it is well known, the normal stress σ_y, for $\theta = 0$, given by the linear elastic fracture mechanics (LEFM) is:

$$\sigma_y = \frac{K_I}{\sqrt{2\pi r}}, \tag{9}$$

in which r is the radial distance from the crack tip and K_I is the stress intensity factor (SIF). For the SEC specimen in Fig. 4 [16], the SIF can be evaluated as follows:

$$K_I = \frac{P}{t\sqrt{W}} \sqrt{7{,}59\frac{a}{W} - 32\left(\frac{a}{W}\right)^2 + 117\left(\frac{a}{W}\right)^3}\,. \tag{10}$$

Eq. (9) shows that the elastic stress would become very large in the proximity of the crack tip. In practice, these large stresses do not occur because this region becomes plastic-like deformed, due to the SIM. It would appear, therefore, that in such materials the deformation zone at crack tip would invalidate the use of LEFM. However, Irwin [17] has shown that when yielding occurs at the crack tip in common metals, LEFM techniques may still be applied if an equivalent crack length is used, *i.e.* a physical crack length plus an allowance for the extent of the plastic zone. This zone is generally represented by a circular boundary radius, r_y, at the crack tip and the effective crack length becomes $a_{eff}=a+ r_y$. For plane stress conditions, *i.e.* $s << W$, r_y is given by:

$$r_y = \frac{1}{2\pi}\left(\frac{K_I}{S_y}\right)^2, \tag{11}$$

where S_y is the yield strength of the material. Thus the size of plastic zone is $r_p=2\ r_y$.
Taking into account r_y, Eq. 9 is modified as follows:

$$\sigma_y = \frac{K_{Ieff}}{\sqrt{2\pi(r - r_y)}}. \tag{12}$$

where K_{Ieff} is the effective SIF obtained substituting a_{eff} into Eq. 10. Irwin correction of LEFM was used herein to analytically estimate the values of r_A on the symmetry plane in front of the crack tip of the NiTi alloy, substituting σ_s^{AM} to S_y in Eq. 11. The comparison between the analytical and numerical results is shown in Table 2. The results show that the analytical solution overestimates the martensite start radius.

Table 2. Analytical and numerical values of r_A for different temperatures.

T [K]	analytical r_A [μm]	numerical r_A [μm]
303	183,1	115,1
308	124,6	79,5
313	90,5	57,5
318	68,8	44,1
323	54,1	34,8
328	43,7	28,6

In Fig. 9, the numerically obtained normal stress, σ_y, *versus* the radial distance from the crack tip, r, is shown in a bi-logarithmic plot, for T=303 K. In this plot, the values for nodes located at a distance r>2 mm were not taken into account, since they are outside the stress singularity zone. Increasing the distance from the crack tip, two knees are clearly visible, corresponding to the martensite finish and start, respectively. Using ordinary least square, the equation of the linear region, in Fig. 9, corresponding to the austenitic zone, was evaluated; in particular, the slope is -0,5,

which corresponds to the theoretical value. Thus, Eq. 12 is capable to describe the normal stress, σ_y, in SMA for $r > r_A$, *i.e.* in the austenitic region, but not within the phase transformation zone. Indeed, the beginning of the phase transformation zone is affected not only by the value of σ_s^{AM}, but also by what happens in front of the crack tip.

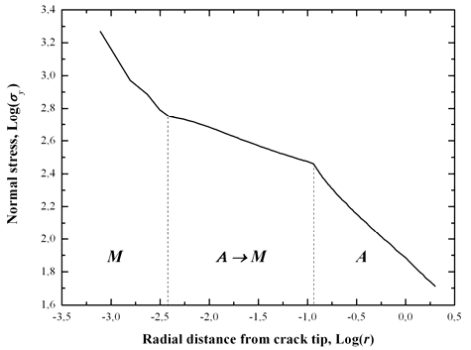

Fig. 9 Normal stress, σ_y, vs. radial distance from crack tip, r (T= 303 K).

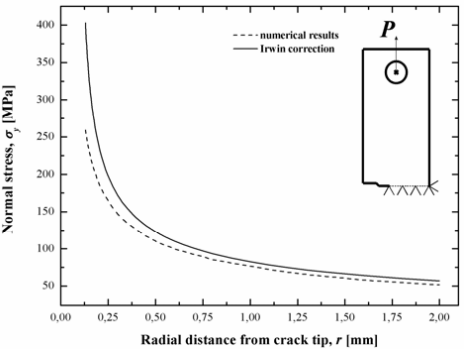

Fig. 10 Normal stress, σ_y, distribution in front of the crack tip (T=303 K).

Finally, Eq. 12 was applied to estimate the stress distribution in the austenitic region and within the stress singularity zone, *i.e.* for $r_A < r < 2$ mm, by using the values of $r_A/2$, that is:

$$\sigma_y = \frac{K_{Ieff}}{\sqrt{2\pi(r - r_A/2)}}. \tag{13}$$

In Fig. 10, a comparison between the numerical results for T=303 K and the theoretical predictions of Eq.13 is shown. The figure shows a similar trend between the two curves, but the differences increases when decreasing the distance from the crack tip. Notwithstanding these differences, the results indicate that the Irwin correction of LEFM could be used to describe the stress distribution in the austenitic region but a proper equation should be found to estimate the effective crack length. In fact, the gap between the curves in Fig 10 can be reduced by moving the vertical asymptote of the Irwin curve, *i.e.* by changing the value of r_y in Eq. 12. Further studies should be carried out in order to define a modified relation for the effective crack length, which takes into account the whole stress-strain curve of the material, *i.e.* by considering the stress distribution in the transformation zone as well as in the full martensitic region.

Conclusions and perspectives

In the present work, 2-D numerical simulations were carried out in order to investigate the effects of the temperature on the stress-strain distributions and on the martensitic transformation zone in the crack tip region of a single-edge crack specimen. In particular, the martensite start and finish contours were evaluated from the numerical results. It was demonstrated that the distributions of martensite volume fraction ξ_M in front of the crack tip can be obtained by the distributions of the equivalent plastic strain. The numerical results, presented herein by contour lines, show that the martensite volume fraction ξ_M in the partial martensite zone gradually decreases with increasing the distance from crack tip. Similar results have been obtained for all the investigated temperatures. Moreover, the numerical results show that both the sizes of the transformation start and finish contours decrease with increasing the temperature; however, the extent of the transformation start contour decreases more rapidly than the finish one, resulting in an overall reduction of the transformation zone with increasing the temperature. Finally, comparisons between numerical and

analytical results, obtained by Irwin's modified linear elastic fracture mechanics relations, were carried out. These comparisons show that the analytical approach could be able to describe the stress field in the crack tip region outside the phase transformation zone, *i.e.* in the austenitic region, but a proper equation should be found to estimate the effective crack length. To this aim, further studies should be carried out.

References

[1] K. Otsuka and C.M. Wayman, in: Shape memory materials, edited by Cambridge University Press, Cambridge, UK (1998).

[2] A. Paiva and M.A. Savi: Math. Problems Eng., art. no. 56876 (2006), p. 1

[3] G. Eggeler, E. Hornbogen, A. Yawnyl, A. Heckmann and M. Wagner: Mater. Sci. Eng. Vol. A378 (2004), p. 24

[4] M. Wagner, T. Sawaguchi, G. Kausträter, D. Höffken and G. Eggeler: Mater. Sci. Eng. Vol. A378 (2004), p. 105

[5] G.B. Rao, J.Q. Wang, E.H. Han, W. Ke: Materials Letters 60 (2006) 779–782

[6] Maria Guiomar de Azevedo Bahia, Roge´rio Fonseca Dias, Vicente Tadeu Lopes Buono: International Journal of Fatigue 28 (2006) 1087–1091

[7] S. Yi and S. Gao: Int. J. Solids Struct. Vol. 37 (2000), pag. 819

[8] S. Yi, S. Gao and L. Shen: Int. J. Solids Struct. Vol. 38 (2001), pag. 4463

[9] K. Gall, N. Yang, H. Sehitoglu and Y.I. Chumlyakov: Int. J. Fract. Vol. 109 (2001), p. 271

[10] G.M. Loughran, T.W. Shield and P.H. Leo: Int. J. Solids Struct. Vol. 40 (2003), p. 271

[11] J.H. Chen, W. Sun and G.Z. Wang: Metall. Mater. Trans. Vol. 36A (2005), p. 941

[12] G.Z. Wang: Mat. Sci. Eng. Vol. A434 (2006), p. 269

[13] G.Z. Wang: Mat. Sci. Eng. Vol. A460-461 (2007), p. 383

[14] F. Furgiuele, C. Maletta, A. Falvo, J.N. Reddy: submitted to Smart Mater Struct (2007)

[15] Y. Jung, P. Papadopoulos and R.O. Ritchie: Int. J. Numer.Meth. Eng. 60 (2004), p. 429

[16] P.P Milella in: Meccanica della Frattura Lineare Elastica ed Elastoplastica, edited by Ansaldo Editore, Genova, Italia (1999) (in italian)

[17] G.R. Irwin: Proc. 7th Sagamore Conf. (1960), p. 4